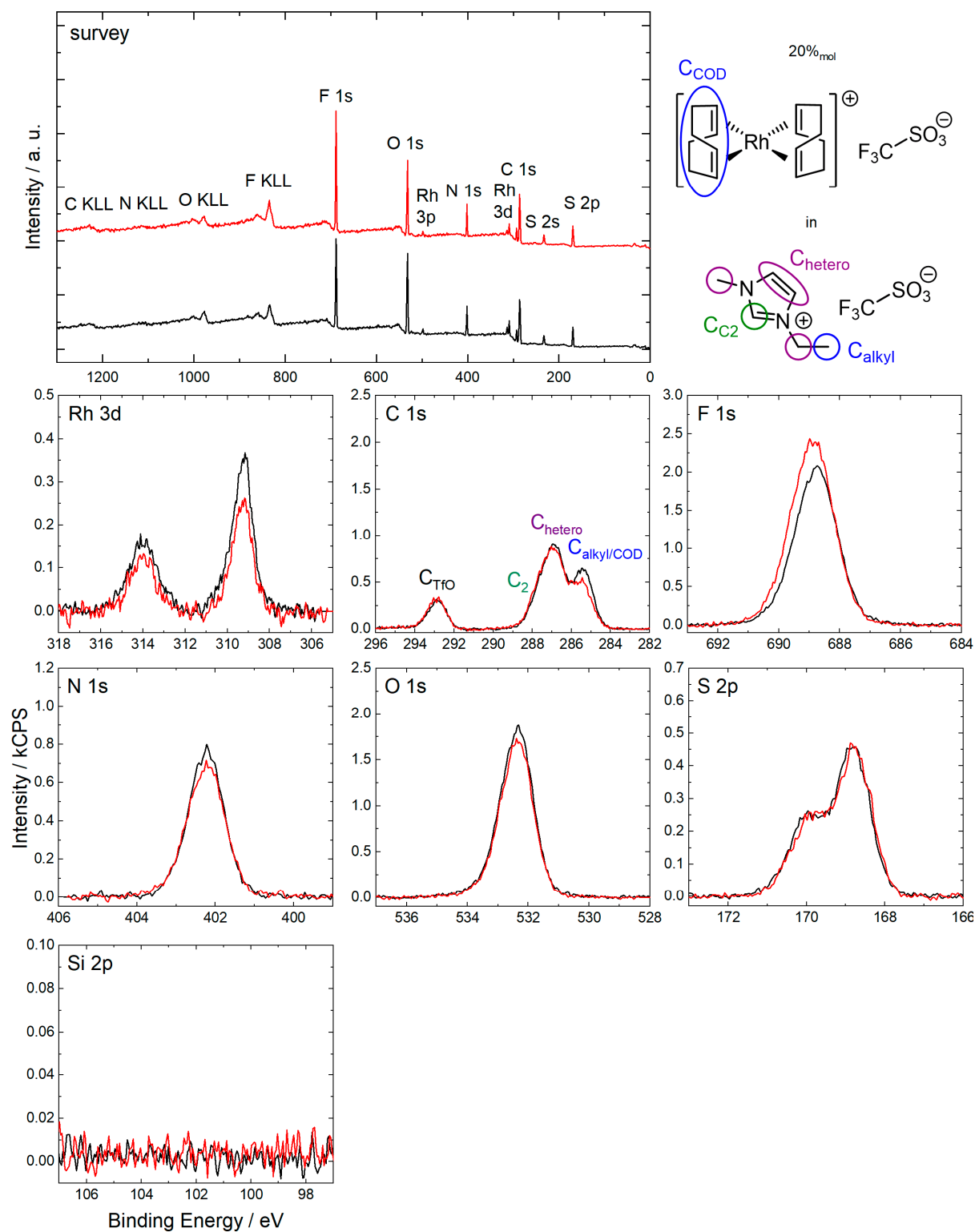


## Structure and Surface Behavior of Rh Complexes in Ionic Liquids Studied by Angle-Resolved X-ray Photoelectron Spectroscopy

by Daniel Hemmeter, Ulrike Paap, Florian Maier, Hans-Peter Steinrück

The supporting information (SI) presents fitting procedures and full sets of all relevant core levels recorded from 20%<sub>mol</sub> solutions of [Rh(COD)<sub>2</sub>][TfO] in [C<sub>2</sub>C<sub>1</sub>Im][TfO] (*figure S1*), [C<sub>4</sub>C<sub>1</sub>Im][TfO] (*figure S6*), [C<sub>8</sub>C<sub>1</sub>Im][TfO] (*figure S8*) and [C<sub>2</sub>C<sub>1</sub>Im][EtOSO<sub>3</sub>] (*figure S10*), as well as a 9%<sub>mol</sub> solution of [Rh(COD)<sub>2</sub>][TfO] in [C<sub>2</sub>C<sub>1</sub>Im][TfO] (*figure S5*) and neat [C<sub>2</sub>C<sub>1</sub>Im][TfO] (*figure S3*), [C<sub>4</sub>C<sub>1</sub>Im][TfO] (*figure S7*), [C<sub>8</sub>C<sub>1</sub>Im][TfO] (*figure S9*) and [C<sub>2</sub>C<sub>1</sub>Im][EtOSO<sub>3</sub>] (*figure S11*). For the neat ILs, the quantitative analysis of the high-resolution region spectra is given (*tables 1, 4-6*). Moreover, ARXPS spectra are shown for a solution of [Rh(COD)<sub>2</sub>][TfO] and TPPTS in [C<sub>2</sub>C<sub>1</sub>Im][EtOSO<sub>3</sub>] with 1:2:31.6 ratio (*figure S14*), for a saturated solution of TPPTS in [C<sub>2</sub>C<sub>1</sub>Im][EtOSO<sub>3</sub>] (*figure S12*, quantitative analysis of 0° spectra in *table S7*) and for a 5.9%<sub>mol</sub> solution of TPPTS in [C<sub>2</sub>C<sub>1</sub>Im][EtOSO<sub>3</sub>] (*figure S13*), that is, a similar TPPTS:IL ratio as in the respective Rh-containing solution (*figure S14*). In all cases, Si 2p spectra are depicted to confirm absence of common surface-active contaminations observed in previous studies[107]. Furthermore, a waterfall plot of Rh 3d spectra (*figure S2*) is shown for a 20%<sub>mol</sub> solution of [Rh(COD)<sub>2</sub>][TfO] in [C<sub>2</sub>C<sub>1</sub>Im][TfO] prepared in air, under full exclusion of air and after more than 100 min of exposure to X-radiation, as well as for solid [Rh(COD)<sub>2</sub>][TfO]. A comparison of O 1s spectra of the 20%<sub>mol</sub> solution of [Rh(COD)<sub>2</sub>][TfO] in [C<sub>2</sub>C<sub>1</sub>Im][TfO] and neat [C<sub>2</sub>C<sub>1</sub>Im][TfO] is further presented (*figure S4*). In addition, details on the different approaches for estimating the loss of COD in the [Rh(COD)<sub>2</sub>][TfO] solutions are presented, together with an overview of the final results (*table S3*). Since the 20%<sub>mol</sub> solution of [Rh(COD)<sub>2</sub>][TfO] in [C<sub>2</sub>C<sub>1</sub>Im][TfO] serves for the exemplary calculation, the atomic sensitivity factor (ASF)-corrected intensities of relevant peaks are given (*table S2*). Finally, the weighed proportions for preparation of the solutions (*table S8*) and other material-related details are shown.



**Figure S1:** Survey, Rh 3d, C 1s, F 1s, N 1s, O 1s, S 2p and Si 2p XPS spectra of a 20%<sub>mol</sub> solution of [Rh(COD)<sub>2</sub>][TfO] in [C<sub>2</sub>C<sub>1</sub>Im][TfO] in 0° (black) and 80° (red) emission recorded at room temperature with assignment of peaks to the molecular structure.

Fitting of the C 1s region was achieved using an established procedure for 1,3-alkylimidazolium based ILs[85]. The contribution of the C<sub>COD</sub> signals is discussed in the main manuscript.

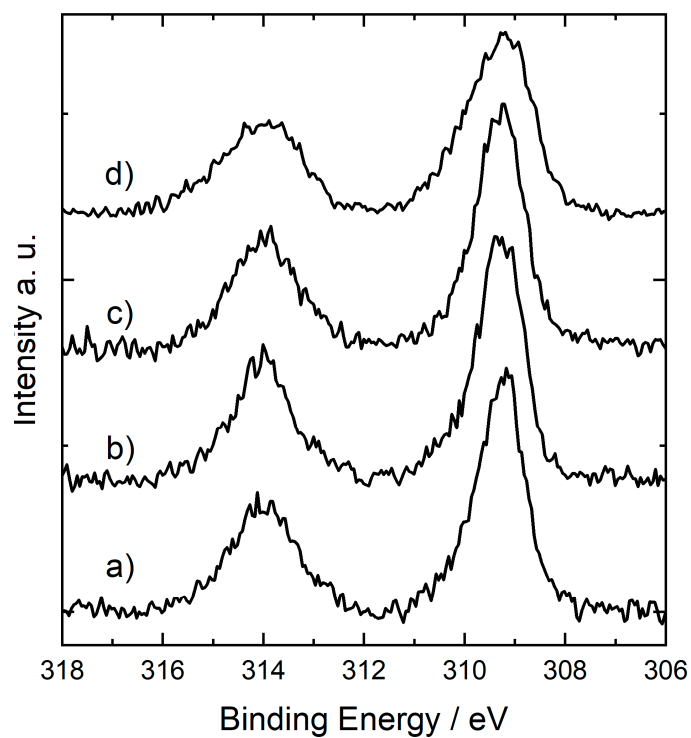


**Figure S2:** Rh 3d XP spectra of 20%<sub>mol</sub> solutions of  $[\text{Rh}(\text{COD})_2][\text{TfO}]$  in  $[\text{C}_2\text{C}_1\text{Im}][\text{TfO}]$  a) prepared in air, b) prepared under exclusion of air, c) solution shown in b) after more than 100 min of X-radiation. d) shows the Rh 3d XP spectrum of the solid catalyst. For sake of comparability, the spectrum shown in d) was referenced to the binding energy of the signal shown in a). Note that the spectrum shown in d) shows broadening due to charging of the solid sample. All spectra were recorded in  $0^\circ$  emission at room temperature.

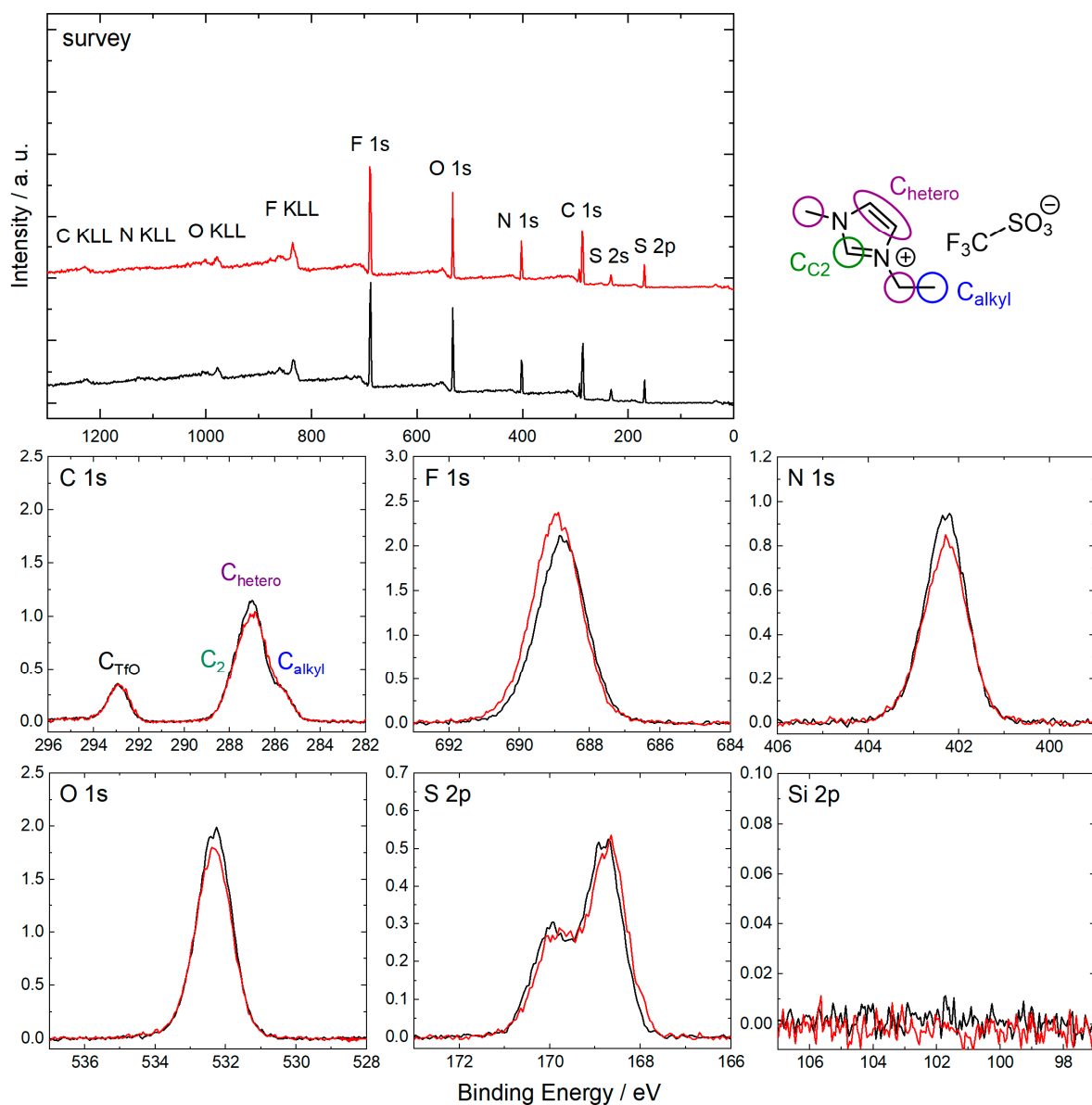


**Figure S3:** Survey, C 1s, F 1s, N 1s, O 1s, S 2p and Si 2p XPS spectra of neat  $[C_2C_1Im][TfO]$  in 0° (black) and 80° (red) emission recorded at room temperature with assignment of peaks to the molecular structure.

Fitting of the C 1s region was achieved using an established procedure for 1,3-alkylimidazolium based ILs[85].

**Table S1:** Quantitative analysis of ARXPS core level spectra of neat  $[C_2C_1Im][TfO]$ .

neat $[C_2C_1Im][TfO]$	C 1s TfO	C 1s $C_2$	C 1s hetero	C 1s alkyl	N 1s	F 1s	O 1s	S 2p
Binding Energy / eV	292.9	287.9	287.0	285.7	402.3	688.8	532.3	169.4
Nominal	1	1	4	1	2	3	3	1
Experimental, 0°	1.1	1.0	3.9	0.9	2.0	3.0	3.1	1.1
Experimental, 80°	1.2	1.0	3.8	0.8	1.8	3.4	2.9	1.1

## Estimation of COD content in solution:

The estimation of the COD contents per metal center in the different solutions is challenging and we thus evaluated three different approaches, the results of which are provided in table S3. In the following, the 20%<sub>mol</sub> solution of [Rh(COD)<sub>2</sub>][TfO] serves as a sample calculation for assessment of the COD content. The ASF-corrected intensities are given in table S2 (see below):

**Approach I:** Assuming full superposition of signals originating from C<sub>alkyl</sub> and C<sub>COD</sub> carbon atoms to give joint C<sub>alkyl/COD</sub> signal.

The expected intensity per atom in the solution was calculated from the sum of ASF-corrected intensities of F 1s, O 1s, N 1s, C<sub>2</sub>, C<sub>hetero</sub> and S 2p signals  $I_j$  divided by the sum of atoms expected from stoichiometric composition  $N_j$  (note that the C<sub>TfO</sub> signal was not involved due to overlaying with the shake-up signal from the aromatic imidazolium ring).

$$I_{per\ atom} = \frac{\sum_{F,O,N,C_2,C_{hetero}} I_j}{\sum_{F,O,N,C_2,C_{hetero}} N_j}$$

With this value, the expected intensity of C<sub>alkyl</sub> carbon atoms  $I_{C_{alkyl}}$  is known (note that the atomic ratios are normalized to one imidazolium cation).

$$I_{C_{alkyl}} = I_{per\ atom}$$

Subtraction from the total intensity of the C<sub>alkyl/COD</sub> signal  $I_{C_{alkyl/COD}}$  yields the intensity of C<sub>COD</sub> carbon atoms  $I_{C_{COD}}$ .

$$I_{C_{COD}} = I_{C_{alkyl/COD}} - I_{C_{alkyl}}$$

The ratio between the ASF-corrected intensity of Rh  $I_{Rh}$  and the calculated intensity of C<sub>COD</sub>  $I_{C_{COD}}$  carbon atoms yields the number of ligand atoms per metal center. This value divided by the number of carbon atoms in one COD ligand (8) yields the number of ligands per metal center  $n_{ligand}$ .

$$n_{ligand} = \frac{I_{C_{COD}}}{I_{Rh}} / 8$$

**Approach I.2:** Alternatively, the contribution of  $C_{alkyl}$  carbon atoms  $I_{C_{alkyl}}$  to the  $C_{alkyl}/COD$  signal can be estimated via the ASF-corrected intensity of the IL-specific N 1s signal  $I_{N_{Im}}$ . The  $[C_2C_1Im]^+$  cation contains half as much  $C_{alkyl}$  atoms than imidazolium nitrogen atoms.

$$I_{C_{alkyl}} = \frac{I_{N_{Im}}}{2}$$

**Approach II:** Assumption of superposition of  $C_{COD}$  with all carbon atoms of the imidazolium cation, that is, chemically differing carbon atoms of the ligand ( $sp^3$  and  $sp^2$  carbon atoms) could appear at different binding energies (between 289 – 284 eV).

The expected intensity of carbon species of the  $[C_2C_1Im]^+$  cation  $I_{C_{C_2C_1Im+}}$  was estimated from the ASF-corrected area of the IL-specific N 1s signal  $I_{N_{Im}}$ . The  $[C_2C_1Im]^+$  cation contains three times more carbon atoms than nitrogen atoms.

$$I_{C_{C_2C_1Im+}} = 3I_{N_{Im}}$$

This intensity was subtracted from the total intensity of the joint envelope (~289 – 284 eV) in the C 1s region to yield the intensity of  $C_{COD}$   $I_{C_{COD}}$ .

$$I_{C_{COD}} = I_{C_{C_2C_1Im+}/COD} - I_{C_{C_2C_1Im+}}$$

The number of COD ligands per metal atom  $n_{ligand}$  was calculated according to the procedure outlined above.

For the  $[C_2C_1Im][TfO]$  solution, all procedures yield 1.4 COD ligands per metal center in solution, as is evident from table S3b. Since the different procedures for estimating the COD content in solution yield similar results, treatment of all ligand atoms and  $C_{alkyl}$  carbon atoms as one peak is valid for  $[C_2C_1Im][TfO]$ , and also for  $[C_4C_1Im][TfO]$ . However, for the  $[C_8C_1Im][TfO]$  solution (table S3d), the different approaches yield variant results: Approaches I and I.2, which are based on the deconvolution of the  $C_{hetero}$  and the  $C_{alkyl}/COD$  peaks, yield a lower COD:Rh ratio than approach II (1.4 and 1.6 vs 2.0). This discrepancy is attributed due to the significant shifting of the  $C_{alkyl}$  signal to lower binding energies upon increasing the chain length (cf. tables S1, S4 and S6). Hence, the peak fitting to deconvolute the  $C_{hetero}$  and  $C_{alkyl}/COD$  peaks under the approach I & I.2 assumption that the  $C_{alkyl}$  and  $C_{COD}$  signals have the same binding energy is less reliable. Consequently, approach II, which is tolerant against different binding energies of  $C_{alkyl}$  and  $C_{COD}$  and does not rely on peak fitting, is considered as the most reliable approach.

**Table S2:** Atomic sensitivity factor (ASF)-corrected intensities obtained from XPS of a 20%<sub>mol</sub> solution of [Rh(COD)<sub>2</sub>][TfO] in [C<sub>2</sub>C<sub>1</sub>Im][TfO] in 0° emission relevant for the calculation of the actual COD content.

20% <sub>mol</sub> [Rh(COD) <sub>2</sub> ][TfO] in [C <sub>2</sub> C <sub>1</sub> Im][TfO]	Rh 3d	C 1s C <sub>2</sub>	C 1s hetero	C 1s alkyl/COD	N 1s	F 1s	O 1s	S 2p
ASF-corrected intensity	136.86	962.64	3850.57	2523.16	1927.52	3638.18	3788.87	1216.36

**Table S3:** Estimation of COD content per metal center in 20%<sub>mol</sub> solutions of [Rh(COD)<sub>2</sub>][TfO] in [C<sub>2</sub>C<sub>1</sub>Im][TfO], [C<sub>4</sub>C<sub>1</sub>Im][TfO], [C<sub>8</sub>C<sub>1</sub>Im][TfO], [C<sub>2</sub>C<sub>1</sub>Im][EtOSO<sub>3</sub>] (a, c-e) and 9%<sub>mol</sub> solution in [C<sub>2</sub>C<sub>1</sub>Im][TfO] (b) using approaches I, I.2 and II outlined above. As the numbers derived from approach II (bold) are the most reliable one, they are used for the further discussion.

		<i>n</i> <sub>ligand,I</sub>	<i>n</i> <sub>ligand,I.2</sub>	<i>n</i> <sub>ligand,II</sub>
a)	9% <sub>mol</sub> [Rh(COD) <sub>2</sub> ][TfO] in [C <sub>2</sub> C <sub>1</sub> Im][TfO]	0.8	0.9	<b>0.8</b>
b)	20% <sub>mol</sub> [Rh(COD) <sub>2</sub> ][TfO] in [C <sub>2</sub> C <sub>1</sub> Im][TfO]	1.4	1.4	<b>1.4</b>
c)	20% <sub>mol</sub> [Rh(COD) <sub>2</sub> ][TfO] in [C <sub>4</sub> C <sub>1</sub> Im][TfO]	1.3	1.3	<b>1.4</b>
d)	20% <sub>mol</sub> [Rh(COD) <sub>2</sub> ][TfO] in [C <sub>8</sub> C <sub>1</sub> Im][TfO]	1.4	1.6	<b>2.0</b>
e)	20% <sub>mol</sub> [Rh(COD) <sub>2</sub> ][TfO] in [C <sub>2</sub> C <sub>1</sub> Im][EtOSO <sub>3</sub> ]	1.1	1.2	<b>1.3</b>

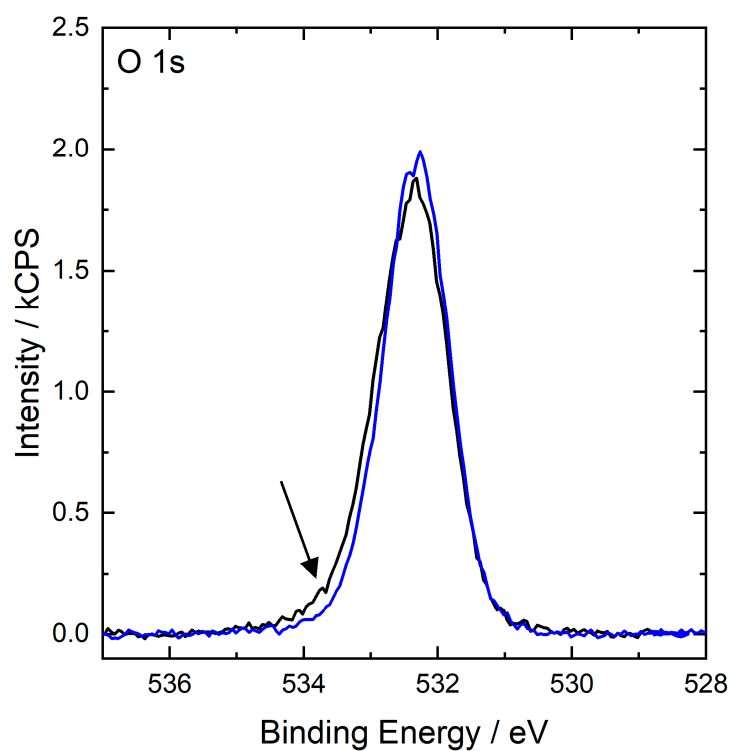


**Figure S4:** O 1s XP spectra of the 20%<sub>mol</sub> solution of [Rh(COD)<sub>2</sub>][TfO] in [C<sub>2</sub>C<sub>1</sub>Im][TfO] shown in figure S1 (black) and neat [C<sub>2</sub>C<sub>1</sub>Im][TfO] shown in figure S3 (blue) in 0° emission recorded at room temperature. The Arrow indicates the additional shoulder in the black spectrum most likely due to [TfO]<sup>-</sup> anions coordinating to the metal center (for details, see main text).



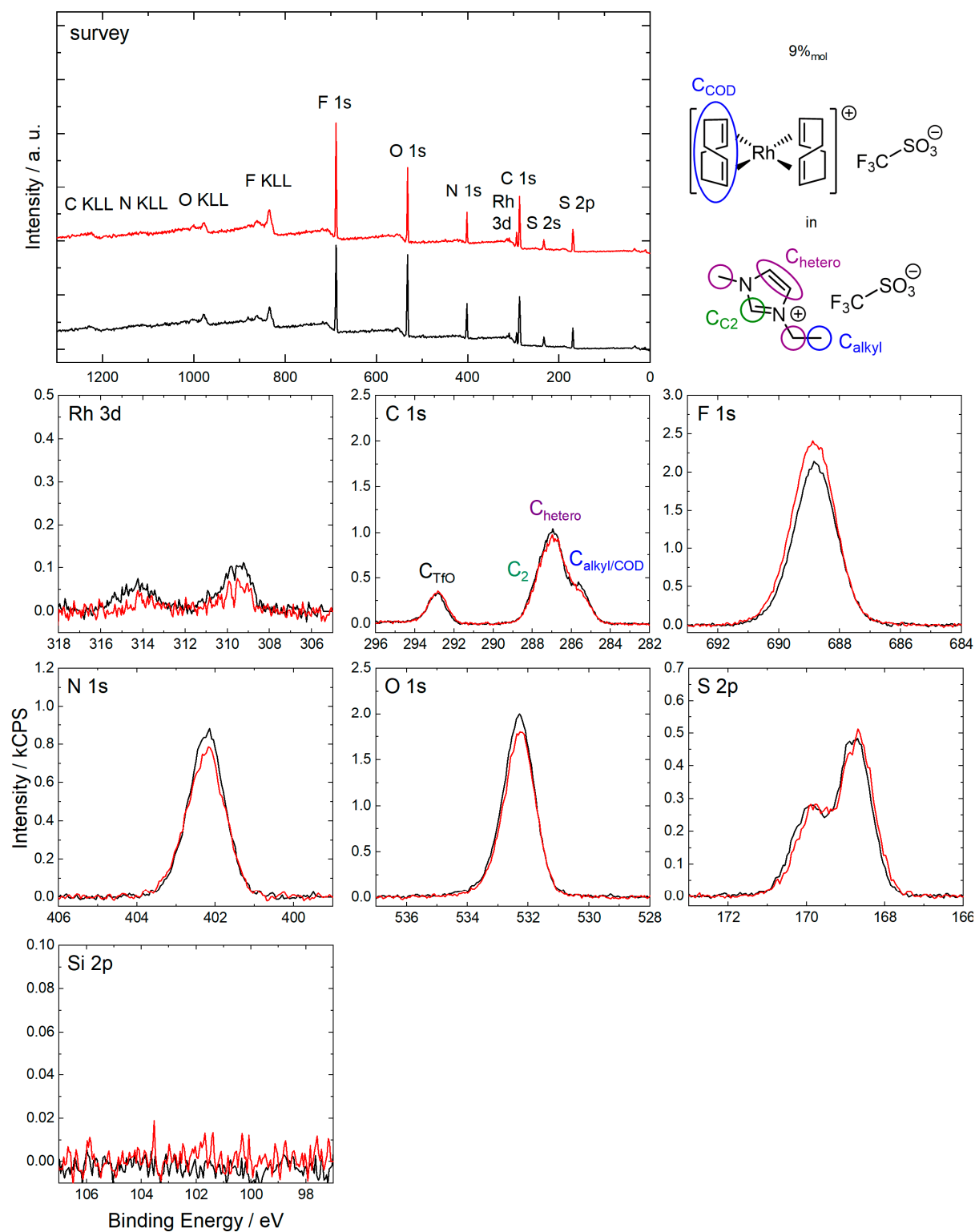


**Figure S5:** Survey, Rh 3d, C 1s, F 1s, N 1s, O 1s, S 2p and Si 2p XPS spectra of a 9%<sub>mol</sub> solution of  $[Rh(COD)_2][TfO]$  in  $[C_2C_1Im][TfO]$  in 0° (black) and 80° (red) emission recorded at room temperature with assignment of peaks to the molecular structure.

For fitting, the same procedure was applied as for the 20%<sub>mol</sub> solution of  $[Rh(COD)_2][TfO]$  in  $[C_2C_1Im][TfO]$  (see above).

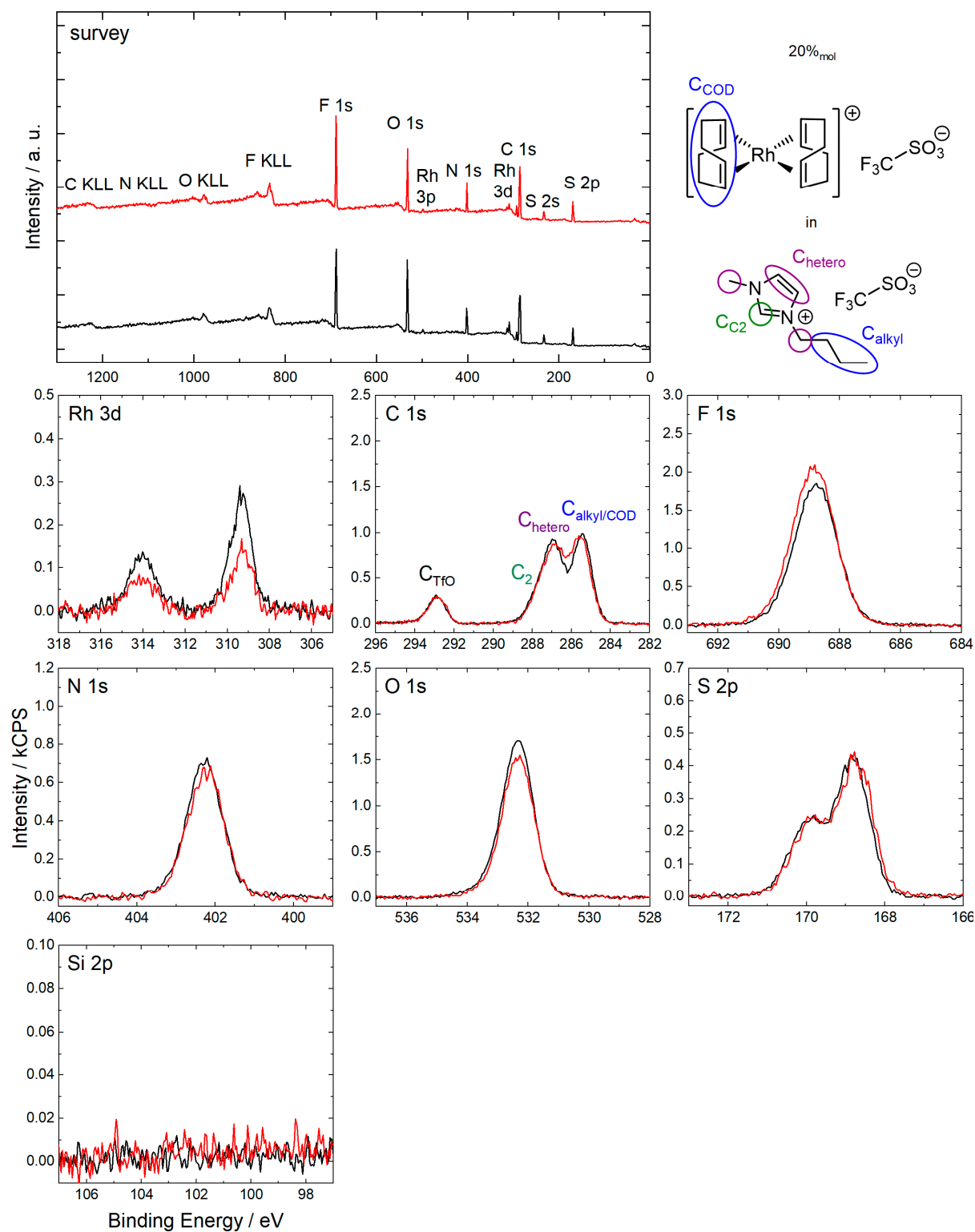


**Figure S6:** Survey, Rh 3d, C 1s, F 1s, N 1s, O 1s, S 2p and Si 2p XPS spectra of a 20%<sub>mol</sub> solution of  $[\text{Rh}(\text{COD})_2][\text{TfO}]$  in  $[\text{C}_4\text{C}_1\text{Im}][\text{TfO}]$  in 0° (black) and 80° (red) emission recorded at room temperature with assignment of peaks to the molecular structure.

For fitting, the same procedure was applied as for the solution of  $[\text{C}_2\text{C}_1\text{Im}][\text{TfO}]$  (see above).

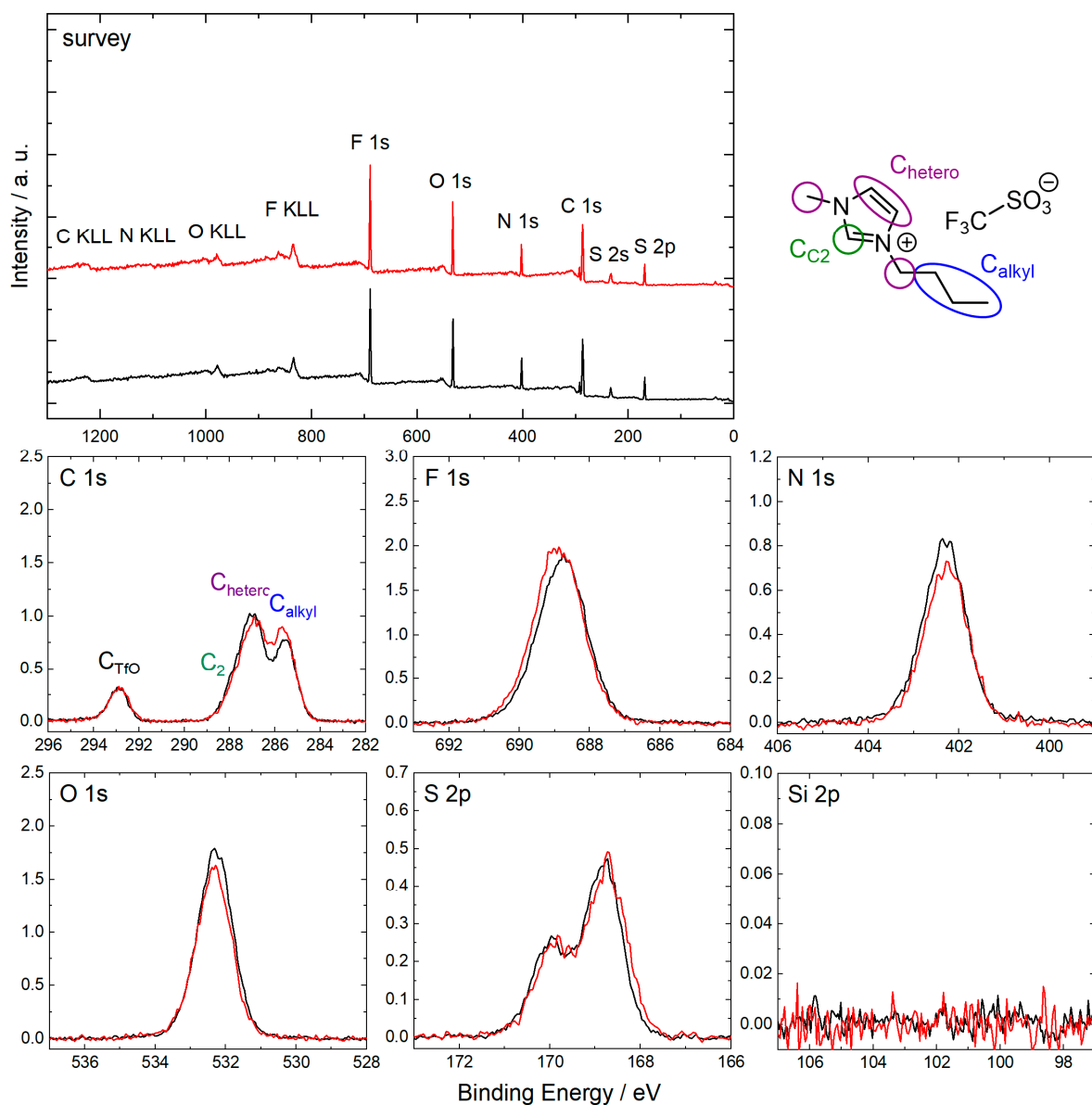


**Figure S7:** Survey, C 1s, F 1s, N 1s, O 1s, S 2p and Si 2p XP spectra of neat  $[C_4C_1Im][TfO]$  in 0° (black) and 80° (red) emission recorded at room temperature with assignment of peaks to the molecular structure.

For fitting, the same procedure was applied as for neat  $[C_2C_1Im][TfO]$  (see above).

**Table S4:** Quantitative analysis of ARXPS core level spectra of neat  $[C_4C_1Im][TfO]$ .

neat $[C_4C_1Im][TfO]$	C 1s TfO	C 1s $C_2$	C 1s hetero	C 1s alkyl	N 1s	F 1s	O 1s	S 2p
Binding Energy / eV	292.9	287.9	287.0	285.5	402.3	688.8	532.3	169.4
Nominal	1	1	4	3	2	3	3	1
Experimental, 0°	1.1	1.0	3.9	2.8	2.0	3.1	3.1	1.1
Experimental, 80°	1.1	0.9	3.8	3.2	1.8	3.3	2.8	1.1

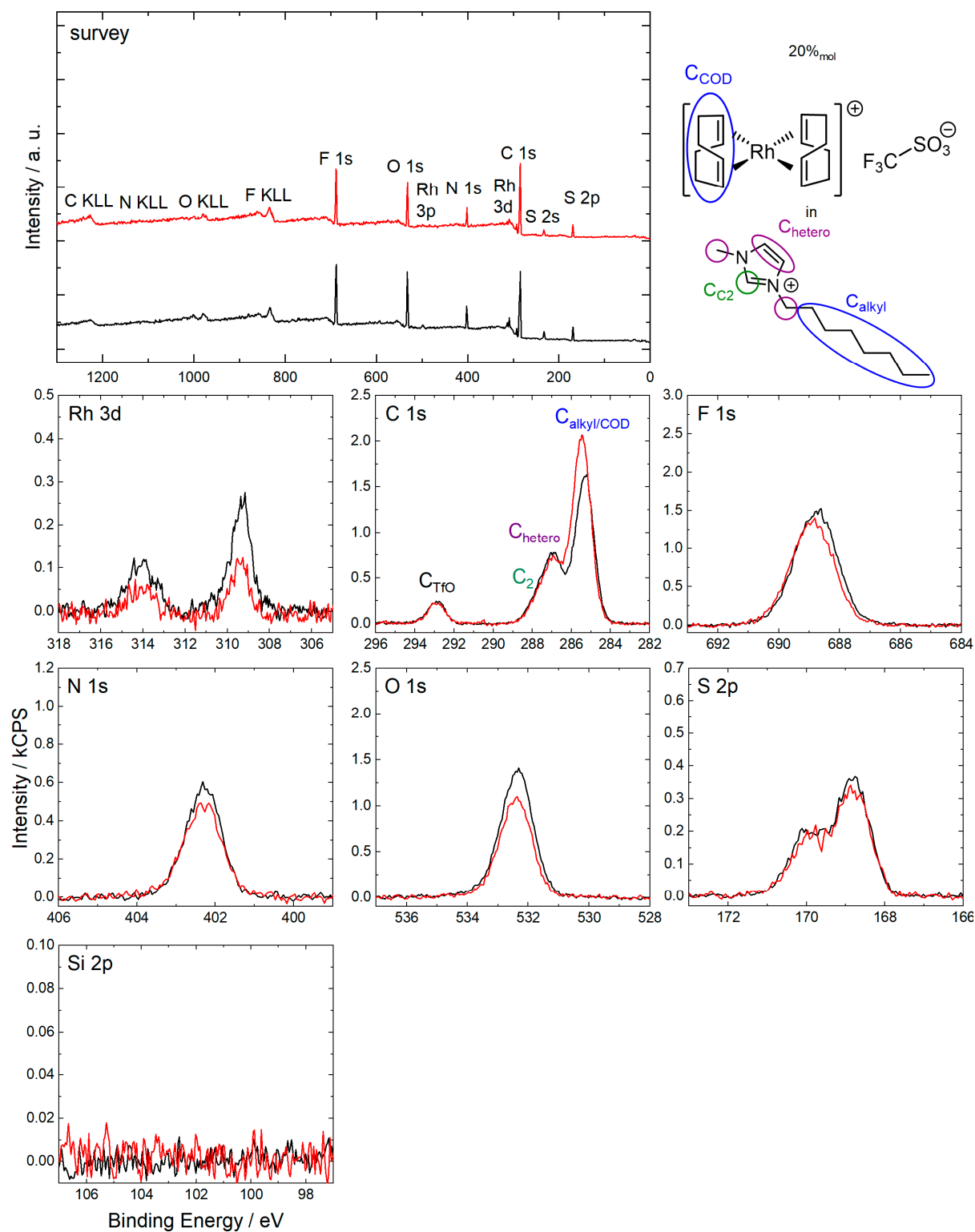


**Figure S8:** Survey, Rh 3d, C 1s, F 1s, N 1s, O 1s, S 2p and Si 2p XPS spectra of a 20%<sub>mol</sub> solution of [Rh(COD)<sub>2</sub>][TfO] in [C<sub>8</sub>C<sub>1</sub>Im][TfO] in 0° (black) and 80° (red) emission recorded at room temperature with assignment of peaks to the molecular structure.

For fitting, the same procedure was applied as for the solution of [C<sub>2</sub>C<sub>1</sub>Im][TfO] (see above).

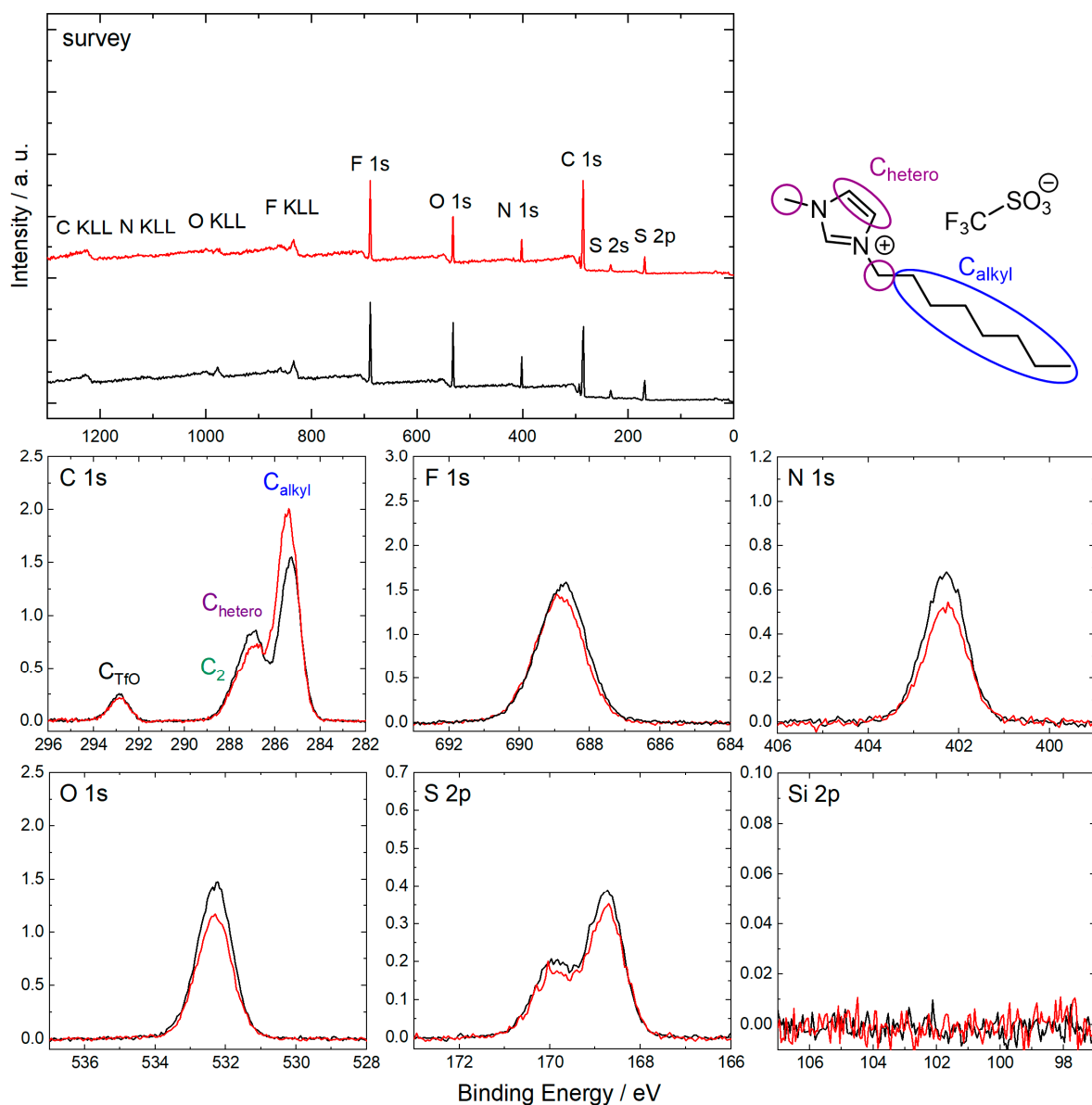


**Figure S9:** Survey, C 1s, F 1s, N 1s, O 1s, S 2p and Si 2p XP spectra of neat  $[C_8C_1Im][TfO]$  in  $0^\circ$  (black) and  $80^\circ$  (red) emission recorded at room temperature with assignment of peaks to the molecular structure.

For fitting, the same procedure was applied as for neat  $[C_2C_1Im][TfO]$  (see above).

**Table S5:** Quantitative analysis of ARXPS core level spectra of neat  $[C_8C_1Im][TfO]$ .

neat $[C_8C_1Im][TfO]$	C 1s TfO	C 1s $C_2$	C 1s hetero	C 1s alkyl	N 1s	F 1s	O 1s	S 2p
Binding Energy / eV	292.9	287.8	286.9	285.3	402.3	688.8	532.3	169.4
Nominal	1	1	4	7	2	3	3	1
Experimental, $0^\circ$	1.0	1.0	4.0	6.8	2.0	3.1	3.1	1.1
Experimental, $80^\circ$	0.9	0.8	3.4	8.9	1.6	2.9	2.5	1.0

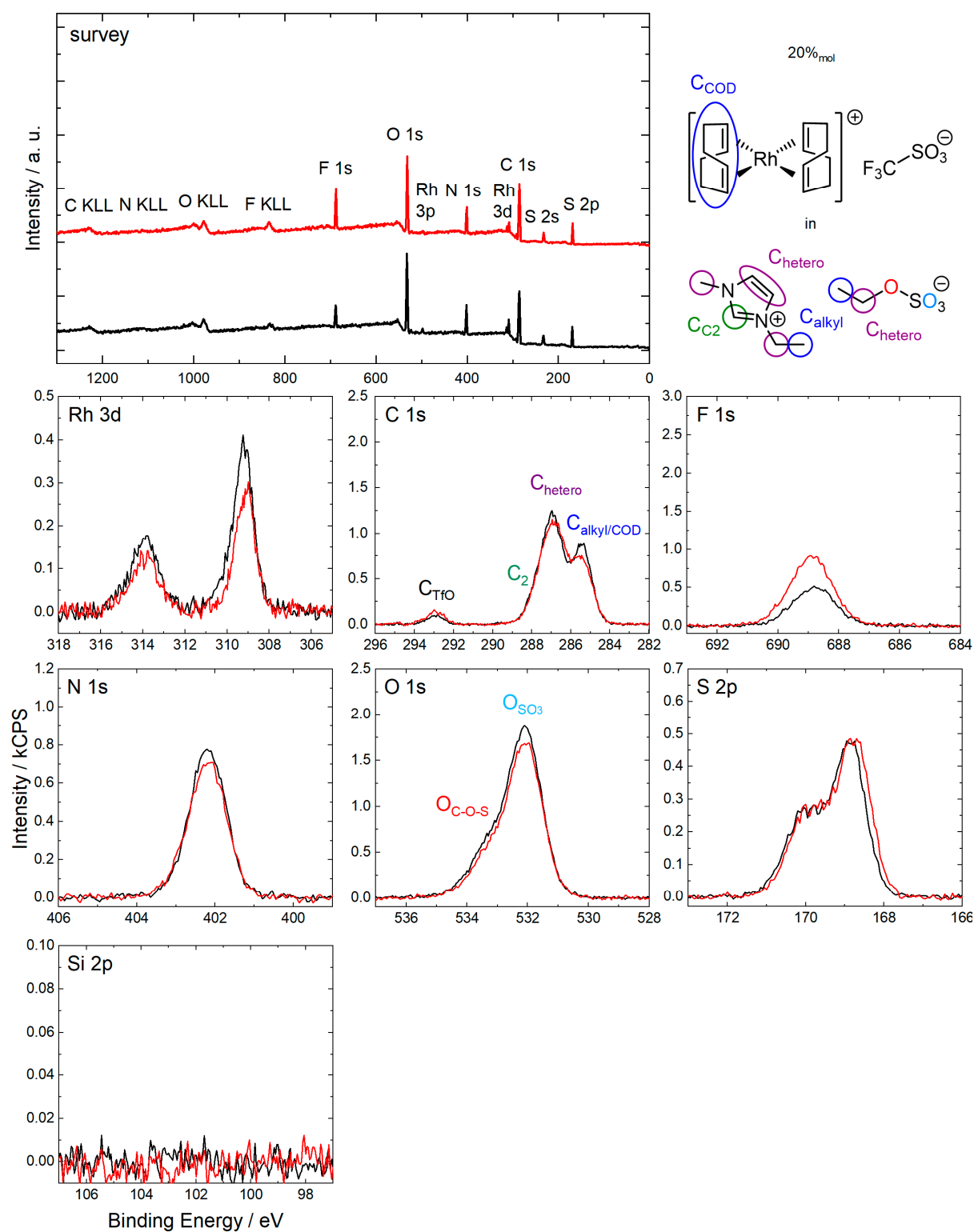


**Figure S10:** Survey, Rh 3d, C 1s, F 1s, N 1s, O 1s, S 2p and Si 2p XPS spectra of a 20%mol solution of  $[Rh(COD)_2][TfO]$  in  $[C_2C_1Im][EtOSO_3]$  in 0° (black) and 80° (red) emission recorded at room temperature with assignment of peaks to the molecular structure.

Fitting of the C 1s region was achieved using an established procedure for 1,3-alkylimidazolium based ILs[85]. In addition, the full width at half maximum (FWHM) of  $O_{C-O-S}$  and  $O_{SO_3}$  signals was set to equal values.

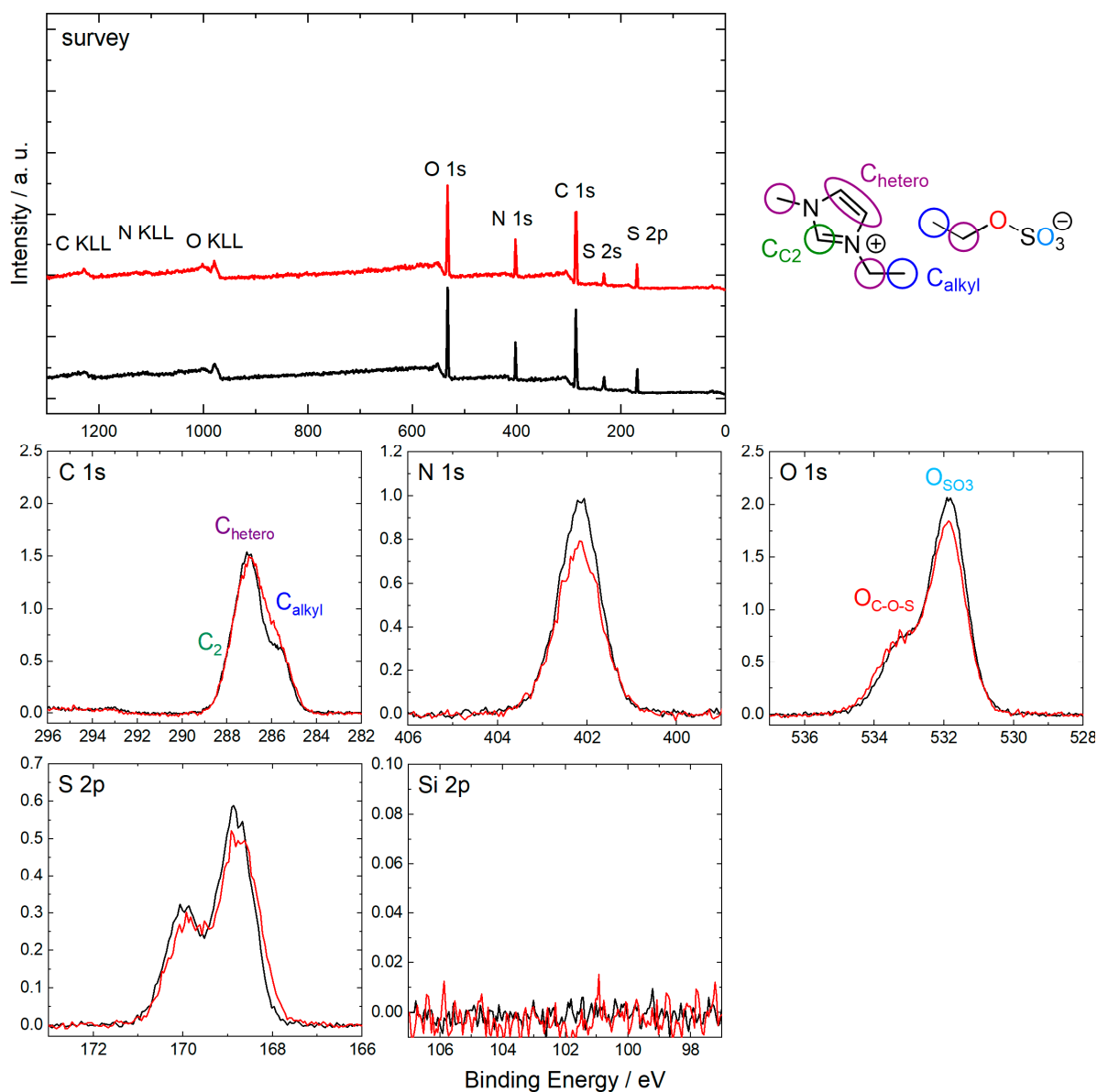


**Figure S11:** Survey, C 1s, N 1s, O 1s, S 2p and Si 2p XPS spectra of neat  $[C_2C_1Im][EtOSO_3]$  in  $0^\circ$  (black) and  $80^\circ$  (red) emission recorded at room temperature with assignment of peaks to the molecular structure.

Fitting of the C 1s region was achieved using an established procedure for 1,3-alkylimidazolium based ILs[85]. In addition, the full width at half maximum (FWHM) of OC-O-S and OSO<sub>3</sub> signals was set to equal values.

**Table S6:** Quantitative analysis of ARXPS core level spectra of neat  $[C_2C_1Im][EtOSO_3]$ .

neat $[C_2C_1Im][EtOSO_3]$	C 1s C <sub>2</sub>	C 1s hetero	C 1s alkyl	N 1s	O 1s C-O-S	O 1s SO <sub>3</sub>	S 2p
Binding Energy / eV	287.9	287.0	285.6	402.2	533.3	531.9	169.4
Nominal	1	5	2	2	1	3	1
Experimental, $0^\circ$	1.0	5.1	1.8	1.9	1.0	3.0	1.1
Experimental, $80^\circ$	1.1	5.3	2.1	1.7	1.1	2.8	1.0

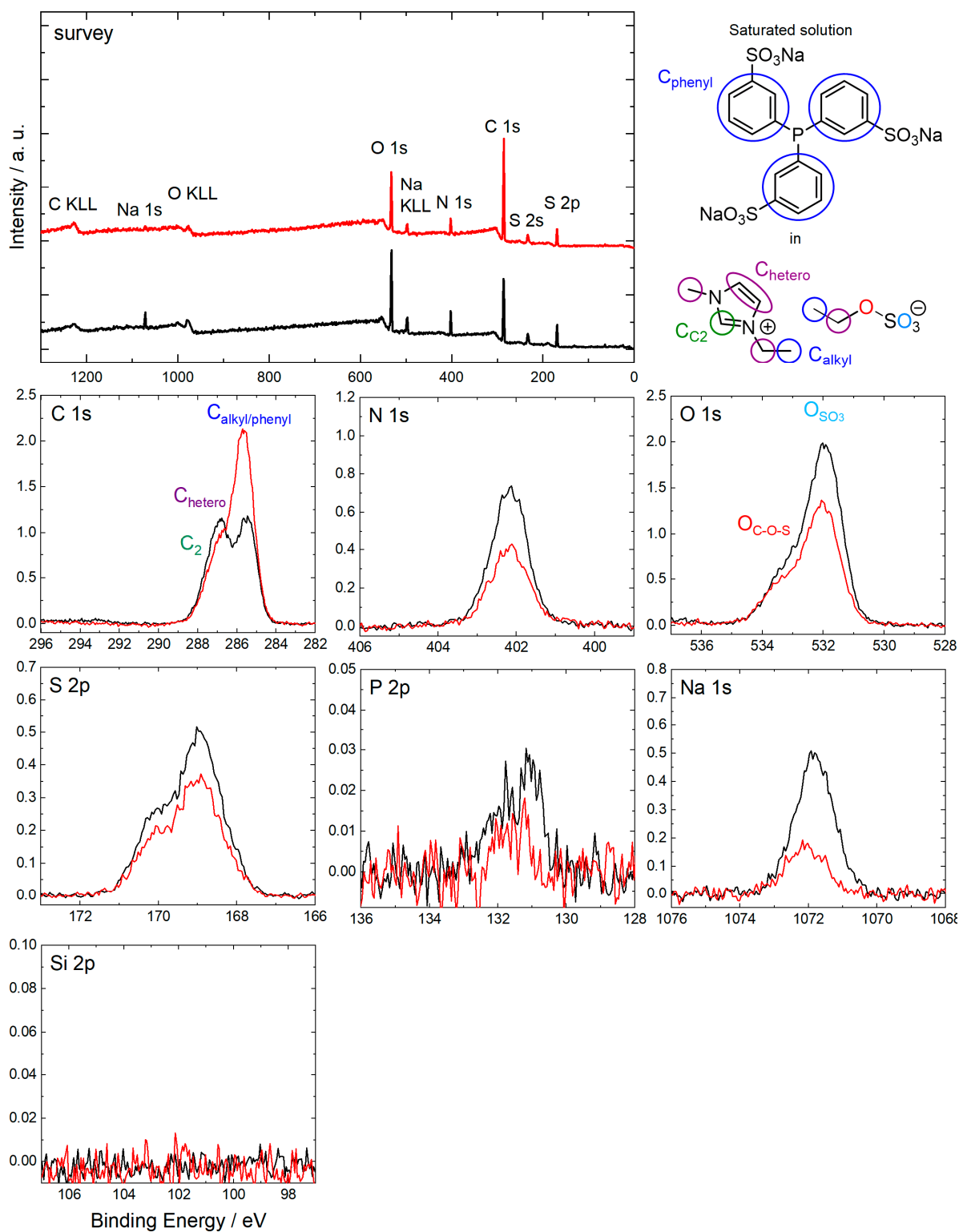


**Figure S12:** Survey, C 1s, F 1s, N 1s, O 1s, S 2p, P 2p, Na 1s and Si 2p XP spectra of a saturated solution of TPPTS in  $[C_2C_1Im][EtOSO_3]$  in 0° (black) and 80° (red) emission recorded at room temperature with assignment of peaks to the molecular structure.

Fitting of the C 1s region was achieved using an established procedure for 1,3-alkylimidazolium based ILs[85]. In addition, the full width at half maximum (FWHM) of  $O_{C-O-S}$  and  $O_{SO_3}$  signals was set to equal values.



**Table S7:** Quantitative analysis of XPS core level spectra recorded in 0° emission of a solution of TPPTS in [C<sub>2</sub>C<sub>1</sub>Im][EtOSO<sub>3</sub>] assuming a solubility of 16.1%<sub>mol</sub>.

Solution of TPPTS in [C <sub>2</sub> C <sub>1</sub> Im][EtOSO <sub>3</sub> ] assuming a solubility of 16.1% <sub>mol</sub>	C 1s C <sub>2</sub>	C 1s hetero	C 1s alkyl/COD	N 1s	O 1s C-O-S	O 1s SO <sub>3</sub>	S 2p	P 2p	Na 1s
Binding Energy / eV	287.8	286.9	285.5	402.2	533.3	532.0	169.5	131.5	1071.8
Nominal	1.00	5.00	5.46	2.00	1.00	4.73	1.58	0.192	0.577
Experimental, 0°	1.07	5.36	5.14	2.06	1.32	4.50	1.61	0.089	0.389

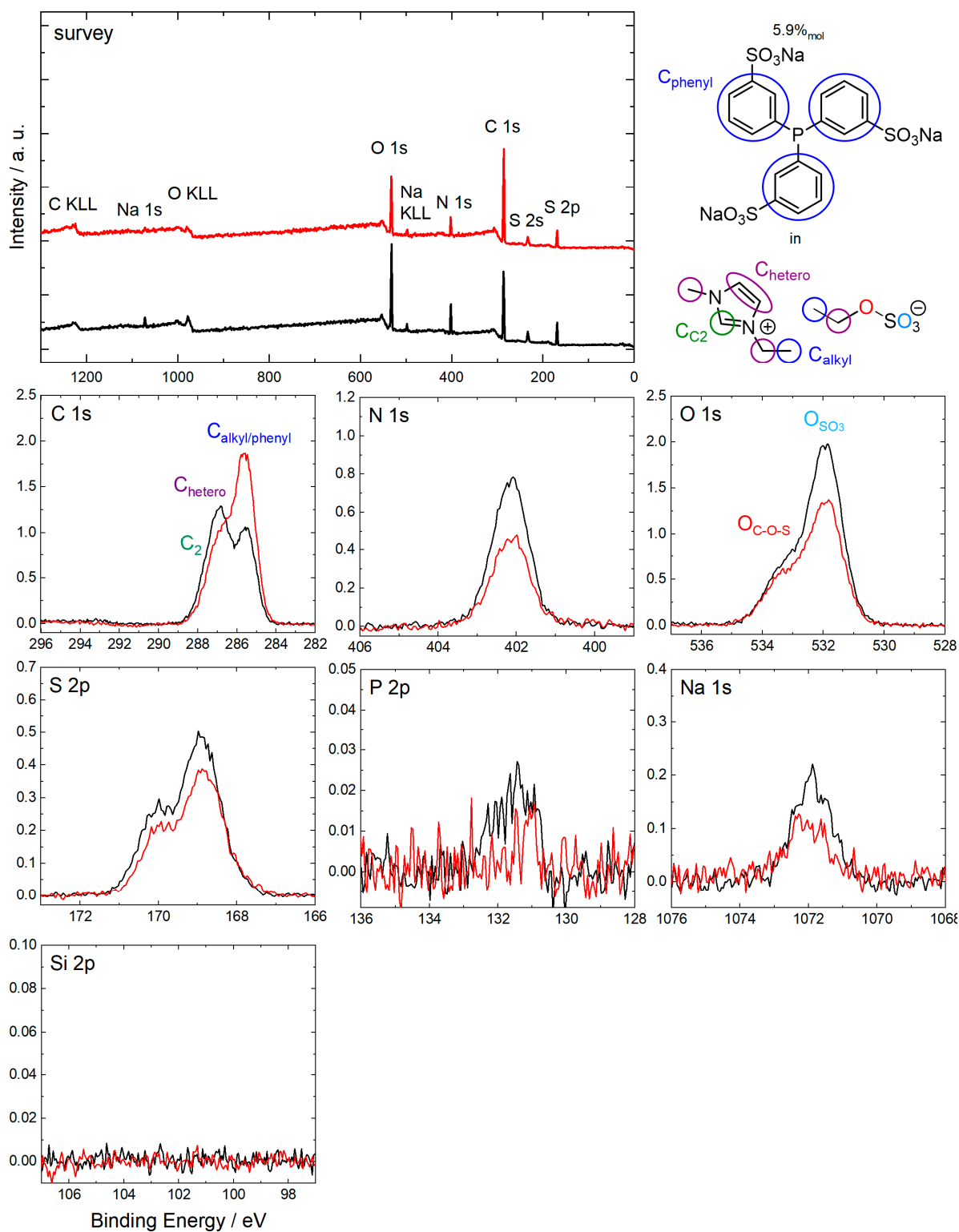


**Figure S13:** Survey, C 1s, F 1s, N 1s, O 1s, S 2p, P 2p, Na 1s and Si 2p XP spectra of a 5.9%<sub>mol</sub> solution of TPPTS in  $[C_2C_1Im][EtOSO_3]$  in 0° (black) and 80° (red) emission recorded at room temperature with assignment of peaks to the molecular structure.

Fitting of the C 1s region was achieved using an established procedure for 1,3-alkylimidazolium based ILs[85]. In addition, the full width at half maximum (FWHM) of  $O_{C-O-S}$  and  $O_{SO_3}$  signals was set to equal values.

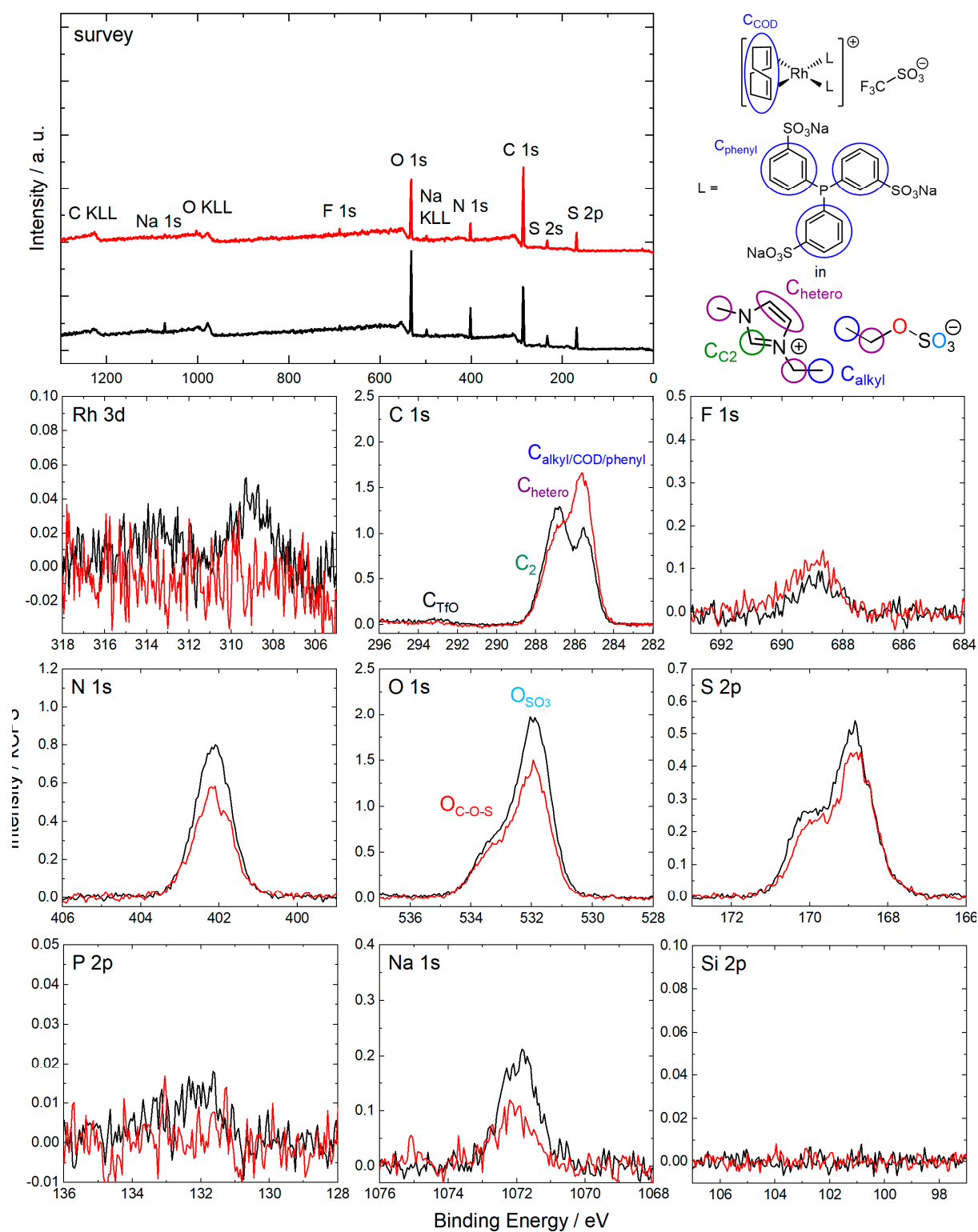


**Figure S14:** Survey, Rh 3d, C 1s, F 1s, N 1s, O 1s, S 2p, P 2p, Na 1s and Si 2p XPS spectra of a solution of  $[\text{Rh}(\text{COD})_2][\text{TfO}]$  and TPPTS in  $[\text{C}_2\text{C}_1\text{Im}][\text{EtOSO}_3]$  with 1:2:31.6 ratio in  $0^\circ$  (black) and  $80^\circ$  (red) emission recorded at room temperature with assignment of peaks to the molecular structure.

Fitting of the C 1s region was achieved using an established procedure for 1,3-alkylimidazolium based ILs[85]. In addition, the full width at half maximum (FWHM) of Oc-o-s and Oso3 signals was set to equal values.

**Table S8:** Weighed proportions for mixtures investigated in this work.

	20%mol [Rh(COD) <sub>2</sub> ][TfO] in [C <sub>2</sub> C <sub>1</sub> Im][TfO]	9%mol [Rh(COD) <sub>2</sub> ][TfO] in [C <sub>2</sub> C <sub>1</sub> Im][TfO]	20%mol [Rh(COD) <sub>2</sub> ][TfO] in [C <sub>4</sub> C <sub>1</sub> Im][TfO]	20%mol [Rh(COD) <sub>2</sub> ][TfO] in [C <sub>8</sub> C <sub>1</sub> Im][TfO]	20%mol [Rh(COD) <sub>2</sub> ][TfO] in [C <sub>2</sub> C <sub>1</sub> Im][EtOSO <sub>3</sub> ]	Saturated solution of TPPTS in [C <sub>2</sub> C <sub>1</sub> Im][EtOSO <sub>3</sub> ] (16.6%mol weigh- in of TPPTS)	Solution of TPPTS in [C <sub>2</sub> C <sub>1</sub> Im][EtOSO <sub>3</sub> ] (5.9%mol weigh-in of TPPTS)	[Rh(COD) <sub>2</sub> ][TfO] and TPPTS in [C <sub>2</sub> C <sub>1</sub> Im][EtOSO <sub>3</sub> ]
Mass [Rh(COD) <sub>2</sub> ][TfO] / mg	126	43.3	119	126	47.8			75.0
Amount of substance [Rh(COD) <sub>2</sub> ][TfO] / mmol	0.264	0.091	0.248	0.263	0.100			0.157
Mass IL / mg	279	241	278	366	95.1	644	1173	1185
Amount of substance IL / mmol	1.06	0.918	0.955	1.05	0.398	2.70	4.92	4.97
Mass [TPPTS] / mg						321	186	188
Amount of substance [TPPTS] / mmol						0.536	0.310	0.314
Exact molar concentration of complex in IL / %mol	20.0	9.0	20.6	20.0	20.1	*	5.9	Assuming full conversion: 3.1
Exact ratio IL:solute	4.0:1	10.1:1	3.9:1	4.0:1	4.0:1	5.2:1	15.8:1	31.6:2:1 (IL:TPPTS:Rh)

\* Solubility of TPPTS in [C<sub>2</sub>C<sub>1</sub>Im][EtOSO<sub>3</sub>] given in literature: 16.1%mol[74]

$M_{[\text{Rh}(\text{COD})_2][\text{TfO}]} = 468.34 \text{ g/mol}$ ,  $M_{[\text{C}_2\text{C}_1\text{Im}][\text{TfO}]} = 260.24 \text{ g/mol}$ ,  $M_{[\text{C}_4\text{C}_1\text{Im}][\text{TfO}]} = 288.29 \text{ g/mol}$ ,

$M_{[\text{C}_8\text{C}_1\text{Im}][\text{TfO}]} = 344.40 \text{ g/mol}$ ,  $M_{[\text{C}_2\text{C}_1\text{Im}][\text{EtOSO}_3]} = 236.29 \text{ g/mol}$ ,  $M_{\text{TPPTS}} = 568.42 \text{ g/mol}$

Purity: [Rh(COD)<sub>2</sub>][TfO]: 98%, [C<sub>2</sub>C<sub>1</sub>Im][TfO]/[C<sub>4</sub>C<sub>1</sub>Im][TfO]/[C<sub>8</sub>C<sub>1</sub>Im][TfO]

[C<sub>2</sub>C<sub>1</sub>Im][EtOSO<sub>3</sub>]: 99%, TPPTS: 95%

## References (numbers according to main manuscript)

- [106] Gottfried, J. M.; Maier, F.; Rossa, J.; Gerhard, D.; Schulz, P. S.; Wasserscheid, P.; Steinrück, H.-P., Surface Studies on the Ionic Liquid 1-Ethyl-3-Methylimidazolium Ethylsulfate Using X-Ray Photoelectron Spectroscopy (XPS). *Z. Phys. Chem.* **2006**, *220* (10), 1439-1453.
- [85] Niedermaier, I.; Kolbeck, C.; Steinrück, H.-P.; Maier, F. Dual analyzer system for surface analysis dedicated for angle-resolved photoelectron spectroscopy at liquid surfaces and interfaces. *Rev. Sci. Instrum.* **2016**, *87*, 045105.
- [74] Kolbeck, C.; Paape, N.; Cremer, T.; Schulz, P.S.; Maier, F.; Steinrück, H.-P.; Wasserscheid, P. Ligand Effects on the Surface Composition of Rh-Containing Ionic Liquid Solutions Used in Hydroformylation Catalysis. *Chem. Eur. J.* **2010**, *16*, 12083–12087.